

## NOVEL CONVECTIVE INSTABILITIES OF LOW- TO MODERATE-PRANDTL NUMBER FLUIDS

Guy Metcalfe

Division of Building, Construction and Engineering  
CSIRO  
Highett, Victoria  
AUSTRALIA

R.P. Behringer

Dept. of Physics and Center for Nonlinear and Complex Systems  
Duke University  
Durham, North Carolina  
USA

### ABSTRACT

Superfluid mixtures have Prandtl numbers tunable between those of liquid metals and water:  $0.04 < Pr < 2$ . Moreover, superfluid mixtures convect as regular fluids, i.e. classical Rayleigh-Bénard convection. With this unique  $Pr$  range and a variable aspect ratio ( $\Gamma$ ) experiment we survey convective instabilities in the largely unexplored space  $0.12 < Pr < 1.4$  and  $2 < \Gamma < 95$ . Among the novel behaviour found in the survey are: Instability competition greatly increases the complexity of convective states, but a heat-pulse method allows state selection. And, as  $\Gamma$  becomes large ( $> 44$ ), the onset of convection changes from stationary to time-dependent. As  $\Gamma$  increases, oscillations arbitrarily close to the onset of convection arise, then give way to large-amplitude irregular fluctuations.

### INTRODUCTION

The dynamics of Rayleigh-Bénard convection (RBC) rolls—convection in a horizontal layer of fluid subject to a destabilizing density gradient—have been one of the most valuable experimental arenas for generating and testing ideas on linear and nonlinear stability, dynamical systems, chaos, and the transition to turbulence. Superfluid mixture convection (SMC) is an analogous but much less studied form of convection that occurs when the density gradient is created in a layer of a dilute mixture of  $^3\text{He}$  in superfluid  $^4\text{He}$ .

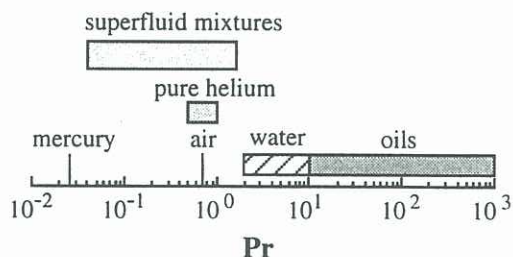


Figure 1: Prandtl number range of fluids commonly used in experiments. Note the large  $Pr$  gap between water and liquid metals bridged by superfluid mixtures.

The prime motivation for using such a novel fluid is the remarkable Prandtl number range available with superfluid mixtures— $0.04 < Pr < 2$ . Over this range the instabilities and dynamics of RBC rolls are expected to change dramatically [3] but no conventional fluid spans this range (fig 1). By expanding the experimental parameter space to areas that previously could only be studied theoretically, this gives SMC the potential to be extremely valuable for research on convective dynamics and stability<sup>1</sup>.

Important parameters governing these instabilities

<sup>1</sup>It is *not* obvious that SMC experiments should be related to RBC calculations, which explicitly assume a classical fluid. See Metcalfe & Behringer [6] for the exhaustive experimental and theoretical justifications and for the caveats.

are the Prandtl number  $Pr$ , which is a ratio of thermal to vortical relaxation times, and the aspect ratio  $\Gamma$ , which governs the geometric arrangement and number of rolls. Other relevant parameters are the Rayleigh number  $Ra$ , the driving force of the flow, and the roll wavevector  $q$ .  $Ra$ - $Pr$ - $\Gamma$  form the experimental control-parameter space. The Nusselt number  $N$  measures the thermal response;  $N - 1$  is the scaled amount of heat carried by convective motion alone<sup>2</sup>.

This paper describes two results from an initial experimental survey of convective dynamics over unexplored regions of  $\Gamma$ - $Pr$  space. The first explores the competitive dynamics around the codimension-2 point where the oscillatory and skew-varicose instabilities intersect. The second observes the onset of convection changing from stationary to chaotic as  $\Gamma$  increases to very large values.

### INSTABILITY COMPETITION

Calculations of the instability boundaries in  $Ra$ - $Pr$ - $q$  space of straight parallel convection rolls have been carried out by Busse & Clever [3]. Two instabilities are relevant for  $Pr \leq 1$ : the stationary, wavelength changing skewed-varicose instability (SVI), which keeps the pattern within the stable band of wavenumbers; and, the time-dependent oscillatory instability (OI), which causes transverse roll oscillations. In the region where the two instability boundaries cross, called a codimension-2 point [5], the instability competition creates a rich complex of multiple stable states. Experimental difficulties had previously prevented codimension-2 points from being fully characterized [7].

We find the crossing point between the OI and the SVI in the range  $0.19 < Pr < 0.29$ . In what follows, the initial wavevector is kept close to its value at onset  $q_c \approx 3.1$ . For  $Pr = 0.19$  the first secondary instability (FSI) is a forward Hopf bifurcation with a frequency in good agreement with theory [3]; for  $Pr = 0.29$  the FSI is the SVI. The agreement between theory and experiment for  $Pr = 0.19$  and  $0.29$  is good, as is to be expected away from the crossing point.

However, in the neighborhood of the crossing the codimension-2 point causes a remarkably complex array of states arises, as seen in the Nusselt data in figure 2 for  $Pr = 0.23$ . At a given  $Ra$ , as many as four different states are accessible. The arrows in figure 2 show the path selected when the heat flux is adiabatically changed. At the FSI the transition is from state A to state D; states B and C are discussed below. Branches A-D and H show only stationary convection. At higher  $r \equiv Ra/Ra_c$  we still find multiple stable states; stationary and time-dependent states may be locally stable at the same  $Ra$ . On branch E, for example, a forward Hopf bifurcation occurs at  $r \approx 2.85$ , but the transition from the stationary

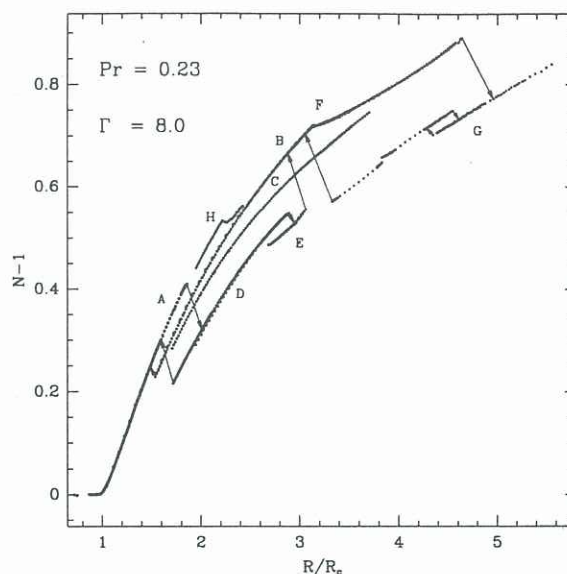


Figure 2: Nusselt curve in the neighborhood of the codimension-2 point, strongly showing the effects of competition between the skewed-varicose and oscillatory instabilities. Branches A-D: steady convection. Branch E: steady for  $r \equiv Ra/Ra_c < 2.85$ , oscillatory otherwise. Branches F, G: time-dependent convection only. Arrows indicate transitions for adiabatically-changed heat current.

branch D is into the middle of the oscillatory region, and shortly after period doubling branch E becomes unstable to branch B. Branch F begins similarly to the true OI, and oscillatory branch F coexists with chaotic branch G. Branch G shows chaos at larger  $r$ ; at lower  $r$  it shows quasiperiodic transitions to chaos, and has other unusual features, such as a hysteresis loop. With decreasing  $Ra$ , branch G makes a transition onto steady branch B. Branch H was brought about by a sudden drop in  $Ra$  which took the system from F to A.

Despite this complexity, the instability realized can be selected with heat pulses. For instance when  $Ra$  is raised by steps along branch A, branch D is selected. On the other hand, if the heat step becomes a heat pulse, short pulses leave the system on A; longer pulses are the same as a heat step; and pulses of in-between duration find branch B or C for narrow, non-overlapping windows of pulse length. Figure 3 shows the Nusselt number obtained after a heat pulse versus the pulse length normalized by  $\tau_v$  the vertical thermal diffusion time. Before each pulse, we arrange the system to be on branch A just below its termination point. The amplitude of the pulse is such that if left on, we always obtain A  $\rightarrow$  D.

The bifurcations near the codimension-2 point unfold with surprising richness. The strikingly complex behavior near the codimension-2 point is due to the competition between the skewed-varicose and oscilla-

<sup>2</sup>Metcalfe & Behringer [6] give precise definitions.



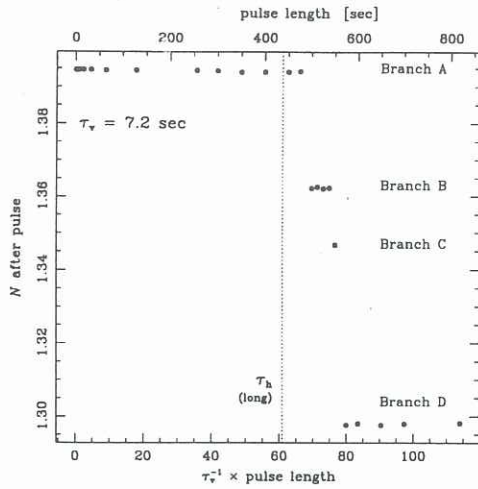


Figure 3: Thermal pulse induced transitions at  $\Gamma = 8.0$ ,  $Pr = 0.23$ . Plotted here is the resulting Nusselt number after the pulse vs. the normalized pulse length. Three steady states (B, C, D) are accessible from state A of figure 2. The amplitude of the pulse is such that leaving it on causes  $A \rightarrow D$ . The vertical dotted line marks the horizontal thermal diffusion time.

tory instabilities, and we emphasize that the Nusselt curve of Figure 2 is *exactly* reproducible to experimental accuracy—and, in fact, most of the branches show overlaying data from several different runs. This rich behavior vanishes away from the codimension-2 point and diminishes with decreasing aspect ratio.

### TRANSITION TO LARGE ASPECT RATIO CONVECTION

What happens at the onset of convection as the aspect ratio is made larger and larger? Of primary interest is whether time-dependence arises *at the onset of convection*. Time-dependence at onset is specifically excluded in infinite- $\Gamma$  calculations [2], and experiments [4] with up to 36 rolls confirm this. But time-dependence has been observed in large fixed- $\Gamma$  experiments [1]. What are the characteristics of this time-dependence and how does it arise with systematic increase in  $\Gamma$ ? We use the variable  $\Gamma$  aspects of our experiment to investigate the changeover from order to disorder at the onset of convection for  $44 \leq \Gamma \leq 90$ ;  $Pr$  is held constant at 1.30. Classically  $\Gamma$  directly indicates the number of rolls; however, superfluid effects reduce the critical wavevector. Longer wavelengths mean fewer rolls.

Our probe for disorder comes from the time-records and power spectra of  $\Delta T$  the temperature difference across the layer. We find three regimes at the onset of convection as  $\Gamma$  increases (fig 4): (1) At smaller  $\Gamma$ , the fluctuations below and above onset are only from instrumental noise. (2) At moderate  $\Gamma$  there is a hysteretic transition to coherent oscillations. Fluctuation amplitude is constant or increases slightly above onset

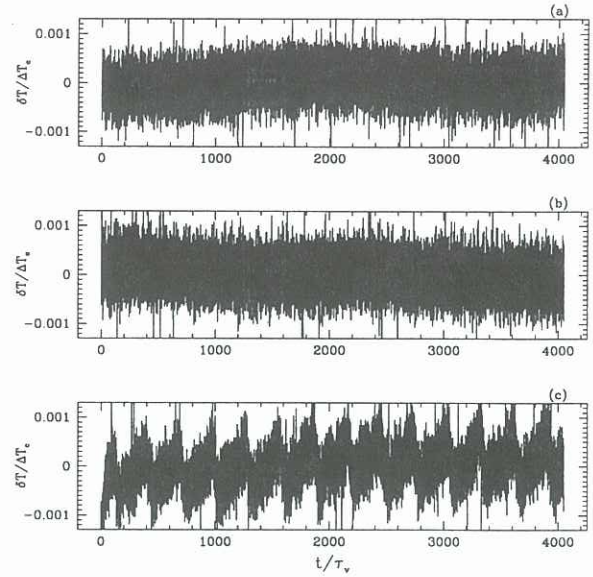


Figure 4: Example time records for  $\Gamma = 70$ . There are 50 rolls. (a) Below onset at  $r = 0.949$ . (b) Fluctuations at  $r = 1.308$ . The signal amplitude in (b) is larger than in (a). (c) Oscillations at  $r = 1.365$ . At this aspect ratio and temperature,  $\Delta T_c = 7.152$  mK and  $\tau_v = 8.35$  sec.

(3) At larger  $\Gamma$ , the fluctuation amplitude increases continuously above onset and is correlated with the Nusselt number. Oscillations cease.

Item 1 affirms our usual picture that onset is steady. Item 3 is similar to the data of Ahlers & Behringer [1] for a  $\Gamma = 57$  cylinder. Item 2 is a new result. There is a regime of aspect ratios between 60 and 85 where coherent oscillations occur near the onset of convection: there is a crossover between ordered, stationary behavior at onset for low  $\Gamma$  and temporal disorder for  $Ra$  arbitrarily close to (but above) the onset of convection for large  $\Gamma$ .

To quantify the growth of the average fluctuation amplitude about  $\Delta T$ , we calculate the integral of the power spectrum or the total power  $P$ . Without oscillations the spectra from which  $P$  is calculated all have the same shape. The spectral shape is flat for several decades with a “knee” frequency near one third of the vertical diffusion time. Above the knee, the spectrum goes as  $f^{-4}$ .

Figure 5 shows plots of  $N$  and  $P$  as functions of  $r$ .  $P$  is normalized by its average value below onset  $P_b$ . The crosses denote  $N$  and go with the left axis; the squares denote  $P/P_b$  and go with the right axis. Filled (open) squares show points with fluctuations (oscillations).

At  $\Gamma = 44$ , we have the behavior expected from steady convection.  $N = 1$  in the absence of convective motion and rises sharply above 1 when convection begins. Thermal fluctuations are the same size

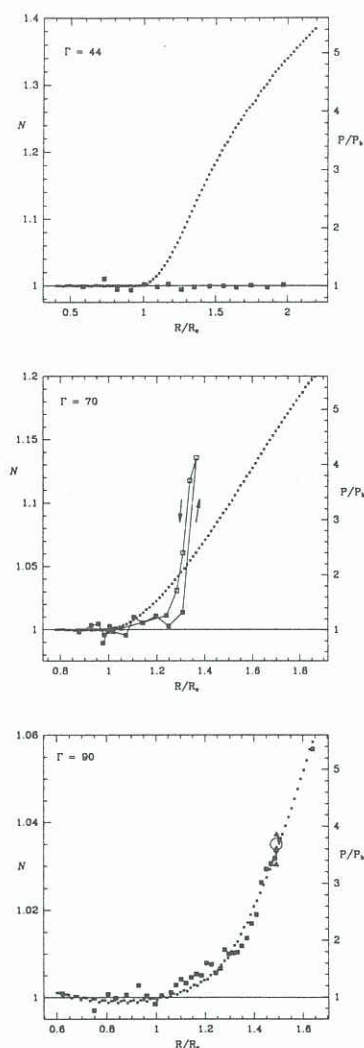


Figure 5: Nusselt number (crosses, left scale) and noise power (squares, right scale) as a function of  $r$  for  $\Gamma = 44$ , 70 and 90 (top, middle, bottom). Open squares denote the presence of a spectral peak. Arrows indicate data taken when raising or lowering  $r$ .

above and below the onset of convection and are due to instrumental noise.

Unexpected behavior begins as  $\Gamma$  increases to 60 and the number of rolls increases to 45. A hysteretic transition to oscillations occurs at  $r \approx 1.7$ . The fluctuation power, though, does not appear to increase above its background level.

With the addition of 5 more rolls ( $\Gamma = 90$ ), the correlation of fluctuation power with Nusselt number becomes apparent. For 58 rolls,  $P$  is linearly correlated with  $N$ . Also at  $\Gamma = 90$  there are no oscillations, as there were at every other aspect ratio above 44.

As the number of rolls at the onset of convection is increased from 36 to 58, there is a changeover from ordered, stationary convection to disordered, time-dependent convection. Between the fully ordered and

fully disordered states there is a crossover region that takes the addition of about 20 rolls to cross. At the beginning of the crossover region there are hysteretic transitions to coherent oscillations near the onset of convection. By the end of the crossover region the amplitude of disordered thermal fluctuations grows proportionally to the Nusselt number, while the onset of oscillations is pushed out to larger  $r$  and is no longer hysteretic. For a large enough number of rolls, the noise power is amplified as soon as a convective velocity field exists, and the fluctuation amplitude is directly proportional to the convective amplitude. About 50 rolls seems to set the length scale at which the interior of the fluid can no longer feel the ordering effects of the sidewalls. We are left with the question of what sets this number?

## FUTURE DIRECTIONS

This initial survey has highlighted the richness and variety of the convective instabilities at low to moderate  $Pr$ . The survey is necessarily incomplete: large regions of  $Pr$ - $\Gamma$  space remained unexplored. Much exploration and characterization remains. Finally, the present experiments have not yielded the convection patterns; information in this regard would be extremely valuable.

## REFERENCES

- [1] Ahlers, G. and Behringer, R.P., 1978, "The Rayleigh-Bénard instability and the evolution of turbulence," *Supp. Prog. Theor. Phys.* **64**, 186–201.
- [2] Chandrasekhar, S., 1961, *Hydrodynamic and Hydromagnetic Stability*, Dover.
- [3] Clever, R.M. and Busse, F.H., 1987, "Nonlinear oscillatory convection," *J. Fluid Mech.* **176**, 403–417.
- [4] Croquette, V., 1989, "Convective pattern dynamics at low Prandtl number: Part I," *Contemporary Physics*, **30**, 113–133.
- [5] Guckenheimer, J. and Holmes, P., 1983, *Nonlinear Oscillations, Dynamical Systems, and Bifurcations of Vector Fields*, Springer.
- [6] Metcalfe, Guy and Behringer, R.P., 1996, "Convection in  $^3\text{He}$ -superfluid- $^4\text{He}$  mixtures. Part I. A Boussinesq analogue," and "Part II. A survey of instabilities," to appear *J. Fluid Mech.*
- [7] Sullivan, T.S. and Ahlers, G., 1988, "Hopf bifurcation to convection near the codimension-two point in a  $^3\text{He}$ - $^4\text{He}$  mixture," *Phys. Rev. Lett.* **61**, 78–81.